BILINGUAL PUBLISHING GROUP

Research in Ecology
https://journals.bilpubgroup.com/index.php/re

ARTICLE

Mapping Vegetation Cover and Assessing Dune Stabilization in the Merzouga Desert Using NDVI Indicators from ASTER and Landsat Data

Naoual El Hammouch [1*], *Hassan Tabyaoui* [1], *Fatima El Hammichi* [1], *Ahmed Gaber* [2]

[1] *Geo-Resources and Environment Laboratory, Sidi Mohammed Ben Abdellah University, Fez 30000, Morocco*
[2] *Faculty of Science, Port Said University, Port Said 42526, Egypt*

ABSTRACT

Desertification and sand dune mobility constitute major environmental challenges in arid regions, particularly in the Merzouga Desert of southeastern Morocco. This study examines the role of vegetation in controlling dune dynamics through a combined analysis of multi-temporal remote sensing data and topographic change detection. Vegetation cover and spatial heterogeneity were evaluated using the Normalized Difference Vegetation Index (NDVI), while sand mobility was assessed using the Normalized Sand Index (NSI) derived from ASTER and Landsat 8 imagery. In addition, geomorphic changes between 2011 and 2025 were analyzed using a DEM of Difference based on ASTER GDEM and Sentinel 1-derived DEMs. The results demonstrate a consistent inverse relationship between vegetation cover and sand mobility across all periods. Vegetated areas, particularly along dune margins, interdune depressions, and oasis environments, are mainly associated with semi-stable dunes and reduced aeolian activity. Even sparse shrub patches significantly contribute to sand trapping and localized dune stabilization. Topographic analysis reveals moderate but spatially organized elevation changes, with sand accumulation on dune crests and windward slopes and erosion on leeward flanks, reflecting dominant regional wind regimes. Central dune fields show relative elevation stability, suggesting a dynamic equilibrium between erosion and deposition. Although classification accuracy decreases in 2025 due to spectral confusion in sparsely vegetated surfaces, qualitative validation using high-resolution Google

*CORRESPONDING AUTHOR:
Naoual El Hammouch, Geo-Resources and Environment Laboratory, Sidi Mohammed Ben Abdellah University, Fez 30000, Morocco; Email: naouallelhammouch@gmail.com

ARTICLE INFO
Received: 19 November 2025 | Revised: 6 January 2026 | Accepted: 20 January 2026 | Published Online: 18 May 2026
DOI: https://doi.org/10.30564/re.v8i3.12800

CITATION
El Hammouch, N., Tabyaoui, H., El Hammichi, F., et al., 2026. Mapping Vegetation Cover and Assessing Dune Stabilization in the Merzouga Desert Using NDVI Indicators from ASTER and Landsat Data. Research in Ecology. 8(3): 136–152. DOI: https://doi.org/10.30564/re.v8i3.12800

COPYRIGHT
Copyright © 2026 by the author(s). Published by Bilingual Publishing Group. This is an open access article under the Creative Commons Attribution-NonCommercial 4.0 International (CC BY-NC 4.0) License (https://creativecommons.org/licenses/by-nc/4.0/).

Earth imagery confirms the reliability of the main spatial trends. Overall, the findings highlight strong vegetation and topography feedbacks that govern dune stabilization processes and provide valuable insights for ecological monitoring and sustainable land management in desert environments.

Keywords: Vegetation Stabilization; Sand Dunes; NDVI; ASTER; Landsat; Desertification; Merzouga; Morocco

1. Introduction

Desertification is widely recognized as one of the major environmental challenges, specifically affecting arid, semi-arid, and dry sub-humid areas worldwide [1]. It is associated with numerous environmental problems, such as soil degradation, salinization [1], sand encroachment, and increased frequency of dust storms, which threaten ecosystems, agricultural productivity, and people's livelihoods [2]. Desertification and deforestation of the landscape have a direct economic and environmental impact. Across the world, land degradation impacts an estimated 1.4 billion people, 74% of whom are poor. Also, in each year, the loss of 12 million hectares of arable land due to drought and desertification is equivalent to 13 million hectares of loss of arable land [3].

Land-degradation is the loss of any land's biological or economic production, resulting in soil degradation, biological degradation, or economic degradation, and/or over time, erosion of natural vegetation [4–6].

The immense ecological problems posed by desertification, with such environmental concerns as soil degradation, soil salinization, silting, and dust storms, have been identified as one of the most pressing concerns of the international community [3].

Desertification is considered an irreversible process caused by natural processes such as temperature, precipitation, vegetation loss, and human processes such as land use/land cover change, industrialization, and urbanization [7–10].

In the desert climate, the main reason for sand dune movement is the lack of vegetative cover. The plants that grow on the sand dune can help stabilize sand [11–13].

Sand dune movement in desert environments is a function of the ecological processes that have underlying processes, such as biotic interactions, seed dispersal, vegetation succession, and environmental change [14–16].

Most of these sand-fixing plants are simple community forms with fewer species and relatively low species content, drought resistant with wind erosion and sand burial resistance, and good wind and sand blocking characteristics [17]. The vegetation of the transition zone can protect the oasis ecosystem from wind and sand erosion and has an important ecological role in ensuring that the organic matter is stable by reducing the flow rate of wind and sand, preventing wind erosion, fixing sand dunes, and enhancing the chemical properties of soil [18].

This requires sustainable management and global perspectives for ecosystem conservation and restoration measures, including the use of remote sensing data. These data, at no additional cost, make it possible to monitor changes in vegetation [19].

The most important biotic components of sand dune habitat are vegetation and the seed bank, which are directly and indirectly related to dune structure stability and resilience [20,21]. Vegetation is a component of a structure in that it allows for accretion and stabilization [22,23]. In desert environments, sand dune dynamics play a key role in land degradation processes [24] due to the mobility of dunes, which can affect infrastructure, agricultural land, and inhabited areas.

Over the past 40 years, various methods of accelerated artificial regeneration have been adopted to promote sand dune stabilization, such as the construction of physical sand barriers and the prohibition of livestock grazing [25]. Thanks to these methods, some mobile dunes can also be gradually restored to become semi-stabilized or stabilized dunes [25].

The stabilization of sand dunes has thus attracted growing scientific interest. From an ecological perspective,

two contrasting approaches coexist with regard to dune stabilization. One favors dune stabilization due to its positive influence on plant diversity [13].

Previous studies have shown that dune stabilization has been implicated in the restoration of degraded vegetation and improving the soil environment [26–28]. Mobile dunes in Horqin Sand Land were characterised by shifting sand, high temperatures, and no water or nutrients available to the soil [29]. Mobile dunes are subsequently artificially stabilized toward semi-fixed dunes and fixed dunes because there is a restoration succession of degraded vegetation, development of biological soil crust, and accumulation of soil nutrients [26–28]. These results also indicate that vegetation cover, species richness, ANPP, soil C, and total N consistently increase with dune stabilization.

In contrast, the second study focused on describing how vegetation change and reduced dune mobility have, or may have, affected dune ecology and geomorphology [30].

In particular, dune sealing has been implicated as a threat to both rare or endangered species as well as decreasing ecological diversity and species richness, often referring to vegetation growth on the front or inside active dunes [31–34].

Dune vegetation plays a crucial role in regulating water migration between the dunes and the interdune lowlands [35,36]. Sand-fixing vegetation significantly limits the movement of soil water in dunes, alters the proportion of each component of the water balance in sandy ecosystems, and reduces the water supplied by dunes to interdune lowlands [37,38].

Understanding how desert species adapt to windy, dry, and sandy environments would accelerate sand fixation speed and reduce the huge economic losses caused by desertification [39].

Many previous studies have analyzed the behavior of sand dunes using geomorphological approaches, remote sensing techniques, and vegetation indices to track dune movements and surface changes [40,41].

Other studies have focused on vegetation distribution and its response to climatic and environmental conditions in desert environments [42–44]. However, these studies have often addressed geomorphological processes and vegetation dynamics separately, without sufficiently integrating their interaction to assess their joint influence on dune stabilization.

Despite the increasing availability of multi-temporal satellite data and advanced GIS tools, the role of vegetation as an agent of sand dune stabilization remains poorly documented, particularly in arid environments. Few studies have proposed a quantitative and integrated assessment of vegetation-induced dune stabilization over extended time periods. This limitation highlights an important research gap addressed by the present study. Thus, the main objective of this work is to evaluate the role of vegetation in sand dune stabilization using a multi-temporal analysis based on remote sensing and geographic information systems (GIS).

This approach aims to improve understanding of the interactions between vegetation and dune dynamics and to contribute to the development of sustainable management strategies for desert environments.

2. Materials and Methods

2.1. Study Area

The study area is located in Merzouga, southeastern Morocco (31°8′49.46″ N, 4°0′34.04″ W). It includes inverted barchanoid dunes and star dunes, classified as complex star dunes [26]. This region is characterized by an arid climate, high temperature variability, and strong seasonal winds that drive the formation and migration of sand dunes. The wind regime is largely bimodal with a SW to NE 210°–240°, Sahel wind known locally as the Sirocco, and an opposing NE-SW 45°–100° Chergui wind with a frequent, but weaker, easterly wind [27]. with very rare precipitation, long and torrid summers, mild and pleasant winters. Rainfall is almost absent all year round, 59 mm in Merzouga [45,46]. The vegetation cover is mainly composed of species such as *Stipagrostis pungens*, the large *perennial grass*, and the *endemic cruciferous Eruca foleyi*. great *tamarisks, Ephedra alata subsp. alenda*. Species that play a crucial role in trapping sand and stabilizing dune surfaces (**Figures 1** and **2**).

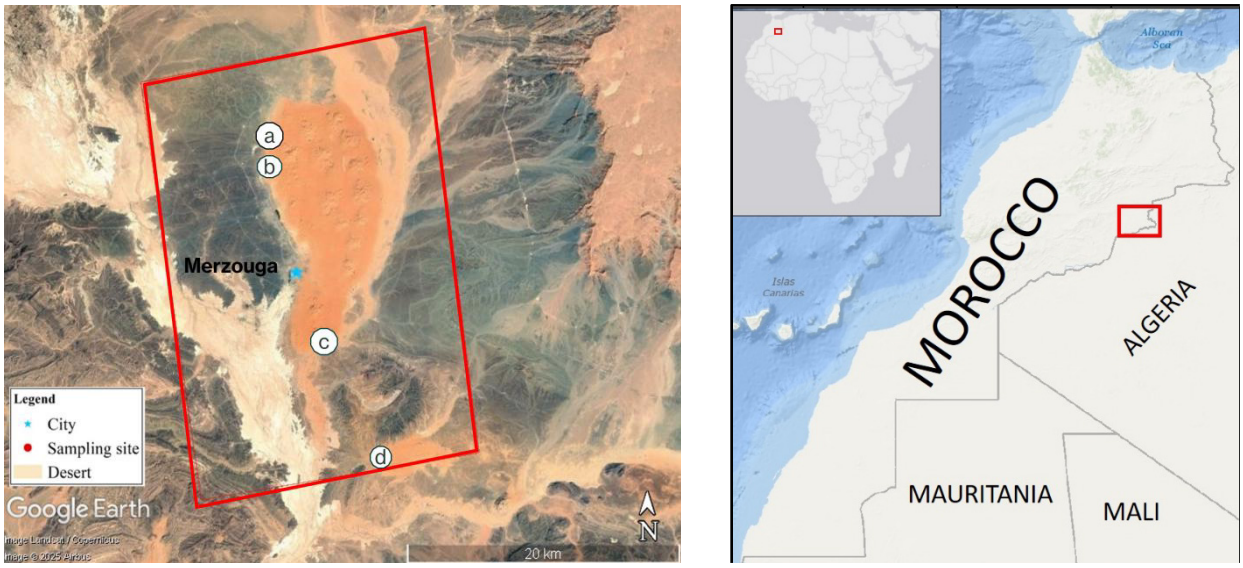

Figure 1. Location of the study area (red rectangles) within the broader region.

Note: letters a,b,c,d in **Figure 1** refer to **Figure 2a–d**.

Source: Atlas-Sahara. Available from: https://atlas-sahara.org/ (in French).

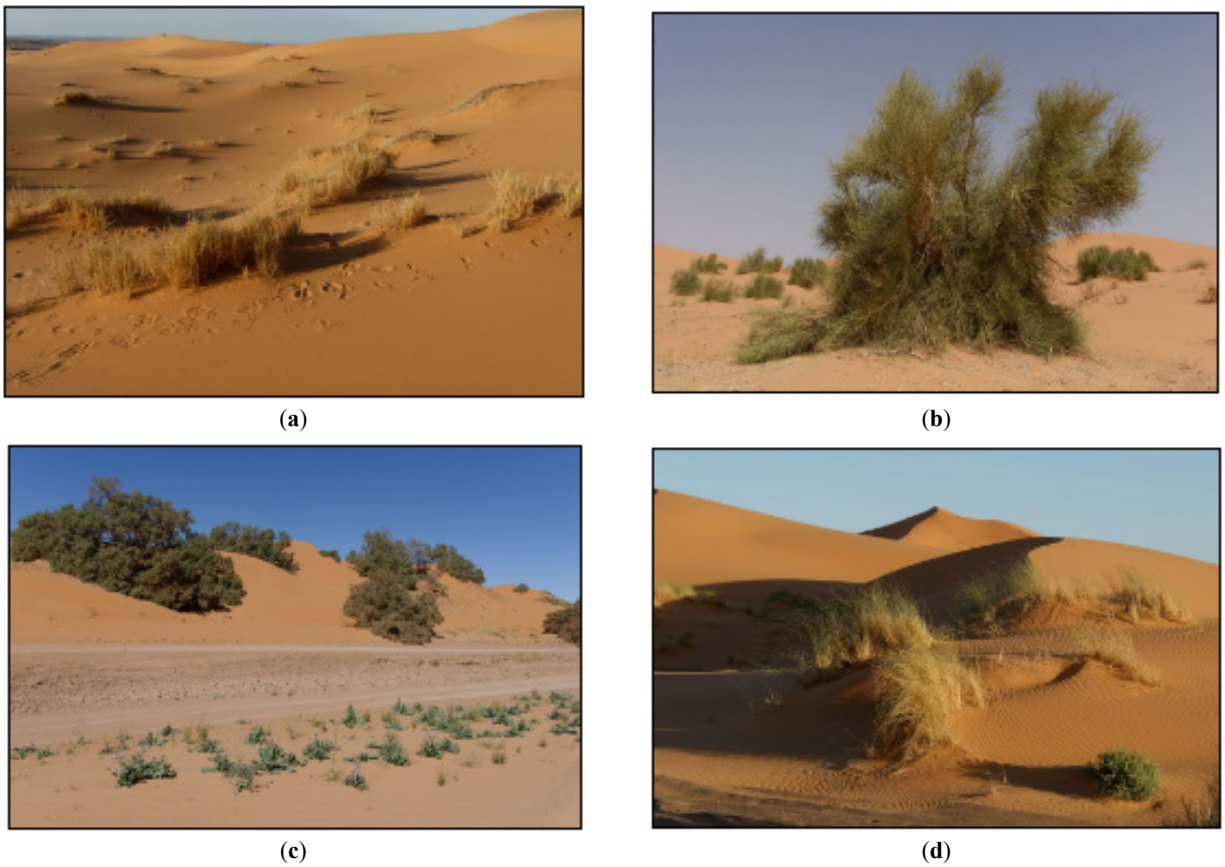

(a) **(b)**

(c) **(d)**

Figure 2. Photographs showing different range land types: (**a**) *Stipagrostis pungens*, the Drinn, is a species of *monocotyledonous* plants of the family Poaceae and the genus Stipagrostis. This large wild grass constitutes vast homogeneous and abundant pastures in the stabilized ergs of the Sahara; (**b**) Mounds of *Stipagrostis pungens*, the great perennial grass of the dunes; (**c**) In the foreground: station of the endemic cruciferous *Eruca foleyi*. In the background: the dry bed of the wadi Talrhemt, which blocks the erg towards the East. In the third plan: the first wooded dunes of great tamarisks. (**d**) *Ephedra alata subsp. alenda* is the most important pioneer plant of the moving and semi-stable sand dunes in the deserts.

2.2. Data Sources

Remote Sensing Data (Landsat-8, ASTER)

Data used in this study included Landsat 8 images acquired on the 1st October 2014 and the 1st October 2025, while ASTER data was acquired on the 26th October 2011. The data was acquired from the United States Geological Survey (https://earthexplorer.usgs.gov/). Attempts were made to acquire images of the same or close dates for consistent comparison between Landsat and ASTER data; however, most of the ASTER data was covered with clouds, and therefore, only available cloud-free data was considered. The study preferred the use of data acquired during the high rainfall summer season when vegetation is denser; however, the unavailability of suitable data necessitated the use of images outside of this time period.

A Sentinel-1 derived DEM was generated using interferometric SAR (InSAR) processing of SAR data acquired in 2025. The ASTER Global Digital Elevation Model (GDEM) acquired in 2011 was used as a reference dataset. Prior to differencing, both DEMs were reprojected to a common coordinate reference system, resampled to a common spatial resolution, and vertically co-registered to reduce systematic elevation biases. A DEM of Difference (DoD) was then produced to quantify topographic changes between 2011 and 2025.

2.3. Data Processing

The image preprocessing involved band combinations, atmospheric correction, and radiometric calibration, which is an important step required to improve the quality of remotely sensed data by removing factors that alter the spectral properties of land surface features [28,45]. Both Landsat and ASTER images were radiometrically calibrated using the absolute calibration method. This enables comparison of images acquired at different times from different sensors [47]. Data was calibrated by firstly converting the digital numbers (DNs) to a sensor spectral. The second step involved converting at-sensor spectral radiance to exoatmospheric top of atmosphere (TOA) reflectance [28]. Equations applicable to Landsat data are explained by Chander et al. [29], while those applicable to ASTER data are provided by Abrams et al. [30], and image clipping. The Basic Tools-Layer Stacking Parameters module of ENVI 5.6. Atmospheric correction was performed using the FLASH module in ENVI 5.6. The images were geo-referenced in the UTM projection and the WGS-84 ellipsoid. Two subsets of VNIR and shortwave infrared (SWIR) bands were used from the 14 available ASTER bands, and subsets of visible, near-infrared (NIR), and shortwave infrared (SWIR) bands were used from the 11 available Landsat 8 OLI bands. We are covering the area of interest, which was processed and analyzed. The Spectral indices, including those for Sand dunes and vegetation, were calculated based on visible and SWIR bands. Supervised classification was carried out on both ASTER (2011) and Landsat 8 (2014–2025) images to map the main land cover types in the Merzouga region. Four classes were identified: stable vegetation, active dunes, semi-fixed dunes, and bare soil. The classification process was based on the Maximum Likelihood algorithm, which has proven effective in arid and semi-arid environments. To assess the performance of the classification, an accuracy assessment was conducted using an error matrix, from which the user's and producer's accuracy were derived for each class. The land cover classifications derived from NDVI for 2011, 2014, and 2025 were validated using high-resolution reference sources and direct field surveys. Field observations were conducted to confirm the spatial distribution of vegetation and mobile sand dunes. In parallel, Google Earth imagery and geological and thematic maps were used to complement and verify the information obtained.

A Digital Elevation Model (DEM) representing surface topography in 2025 was generated from Sentinel-1 Synthetic Aperture Radar (SAR) data using interferometric SAR (InSAR) processing implemented in the SARscape software environment. Sentinel-1 Single Look Complex (SLC) image pairs acquired in 2025 were selected based on orbit consistency, acquisition geometry, and temporal proximity to minimize decorrelation effects. The InSAR workflow included precise orbit correction, radiometric calibration, and accurate co-registration of the master and slave images to ensure sub-pixel alignment. Interferograms were generated by computing the

phase difference between the SAR image pairs, followed by adaptive filtering to reduce phase noise while preserving geomorphological signals. Phase unwrapping was applied to retrieve continuous phase information, which was subsequently converted into elevation values using the sensor's orbital parameters and imaging geometry. The resulting Sentinel-1-derived DEM reflects surface elevation conditions for 2025, with sensitivity to surface roughness and coherence characteristics that are typical of arid dune environments.

The reference elevation dataset consisted of the ASTER Global Digital Elevation Model (GDEM, Version 3) acquired in 2011 and downloaded from the NASA Earthdata platform. The ASTER GDEM provides near-global coverage at approximately 30-m spatial resolution and is derived from optical stereo imagery. Prior to analysis, the ASTER DEM was visually inspected to identify known artifacts such as striping, voids, or anomalous elevation values, which can occur in desert environments due to low surface texture and illumination effects. Minor preprocessing operations were applied where necessary to reduce noise while preserving the overall dune morphology.

To ensure spatial comparability between the Sentinel-1 DEM (2025) and the ASTER GDEM (2011), both datasets were harmonized before elevation differencing. First, the DEMs were reprojected into a common coordinate reference system (WGS 84/UTM zone corresponding to the Merzouga Desert). Second, both DEMs were resampled to a common spatial resolution using bilinear interpolation in order to minimize interpolation artifacts and maintain consistency in grid structure. Vertical co-registration was then performed in ArcGIS to reduce systematic elevation biases arising from differences in sensor geometry and acquisition principles. Stable, non-dynamic reference areas located outside active dune fields, such as consolidated or rocky surfaces, were used to estimate and correct relative vertical offsets between the DEMs. Despite these corrections, residual vertical uncertainties are unavoidable due to differences between optical stereo and SAR interferometric elevation retrieval methods.

Following preprocessing and co-registration, a DEM of Difference (DoD) was generated in ArcGIS by subtracting the ASTER GDEM (2011) from the Sentinel-1 derived DEM (2025). The resulting DoD represents relative elevation changes over the 2011–2025 period. Positive values indicate areas of apparent elevation gain, interpreted as zones of sand accumulation, while negative values indicate apparent elevation loss, interpreted as erosion or sediment redistribution. The DoD was primarily used to analyze spatial patterns of topographic change rather than to quantify absolute volumetric changes. No explicit level of detection (LoD) threshold was applied; therefore, small elevation differences may partly reflect residual noise or sensor-related uncertainty.

It is important to emphasize that this DoD analysis integrates DEMs derived from fundamentally different sensors and acquisition principles. Sentinel-1 SAR measurements are sensitive to surface scattering mechanisms influenced by roughness and moisture, whereas ASTER optical stereo measurements depend on surface texture and illumination conditions. The DoD results provide a reliable indication of relative spatial trends in dune-scale topographic change, capturing key patterns of elevation dynamics over time. The applied processing workflow offers a consistent, reproducible, and robust framework for investigating long-term patterns of aeolian sediment redistribution in the Merzouga Desert, enabling meaningful insights into dune mobility and landscape evolution.

2.4. Normalized Sand Index (NSI)

Normalized Sand Index (NSI), which is calculated based on the Red (R), Green (G), and Short-wave Infrared (SWIR1) bands (Equation (1)). In order to minimize the differences induced by atmospheric and moisture conditions between images collected in different time periods, the sand index values were max–min normalized, resulting in the linear transformation of the data in the range 0–1, which preserves the relationships among the original data values. The application of normalization is a widely used method that restricts a large range of values

to a small range (e.g., 0–1). Under these conditions, we can compare images from different years or results from different indices, applied to the same type of surface (e.g., sand) [46–48].

$$NSI = (G + R)/(\log(SWIR1)) \quad (1)$$

NSI is an index that can be used in the temperate zone, where bare sands and soils have different moisture values. For example, in a major riverbed, soil moisture is higher than on the slopes, and the soil is covered with vegetation. NSI applied to satellite imagery from 2019 maps these details better than NDSAI. Under these conditions, NSI is able to map sandy surfaces without being influenced by moisture. NSI does not generate confusion between light-coloured concrete irrigation channels or other surfaces (e.g., roads) and sand bars [49].

The Normalized Difference Vegetation Index (NDVI) is the most commonly used vegetation index. The NDVI is obtained with Equation (2) [50]. This formula involves the red and near-red bands of each scene. The numbers of these spectral reflectances are different for different satellites, but the wavelengths are almost identical for the red and near-red bands, respectively.

$$NDVI = (NIR-R)/(NIR + R) \quad (2)$$

The atmospheric noise of NDVI due to clouds, dust as well as aerosol is usually found to be negatively biased. This is because additive path radiance enhances the red reflectance whereas less atmospheric transmission reduces the near-infrared reflectance to the effect of systematic underestimation of vegetation indices [51,52]. Recent developments of joint-modeling methods consider this negatively skewed atmospheric pollution specifically to recreate high-quality NDVI time series [53]. Methods of cloud removal and composing have been created to alleviate such errors, especially on the high frequency satellite images [54].

The vegetation indices continue to be the instruments of gold in understanding the temporal relationship of productivity and phenology of the terrestrial ecosystems [55–57]. Their uses in trend detection, land surface phenology extraction and assimilation into vegetation models have been comprehensively reviewed in order to monitor productivity [57,58]. Nonetheless, the presence of the inter-sensor variation in NDVI values may have an impact on the accuracy of the phenological metrics, which underlines the importance of attentive sensor choice and cross-calibration.

The temporal analysis of vegetation indices covers a spectrum of scales, from simple comparisons of two images to time series of multi-decadal time series over 10 years [57,58]. The use of long-term studies based on almost 20 years of observations made on a daily basis has been found to be efficient in the identification of phenological patterns and changes in the dynamics of the ecosystems. These time series are also commonly used in mapping vegetation phenology across a variety of landscapes and biomes, but with special software packages offering full workflows of quality control, fitting, and nursery metric recovery of noisy satellite data [52].

This study investigates the role of vegetation in stabilizing sand dunes in the Merzouga region by analyzing Normalized Difference Vegetation Index (NDVI) data derived from satellite imagery. NDVI is a widely used indicator of vegetation health and coverage, calculated from the red and near-infrared (NIR) spectral bands. In this work, NDVI data were obtained from both ASTER (Advanced Spaceborne Thermal Emission and Reflection Radiometer) and LANDSAT 8 (Operational Land Imager and Thermal Infrared Sensor) satellites, covering the period from (specify years, e.g., 2011–2025).

High NDVI values indicate dense and healthy vegetation, while low values suggest that one is surrounded by or absent from vegetation. In order to narrow the distinction between stable and mobile dunes, threshold values were calculated using NDVI distribution, field observations, and high-resolution Google Earth imagery. Spatial analysis was conducted using Envi 5.6 and ArcGIS 10.8, which was utilized to map vegetation cover and identify areas contributing to dune stabilization. This methodology provides a quantitative assessment of the contribution of vegetation to the mitigation of sand mobility and desertification in Merzouga (**Figure 3**).

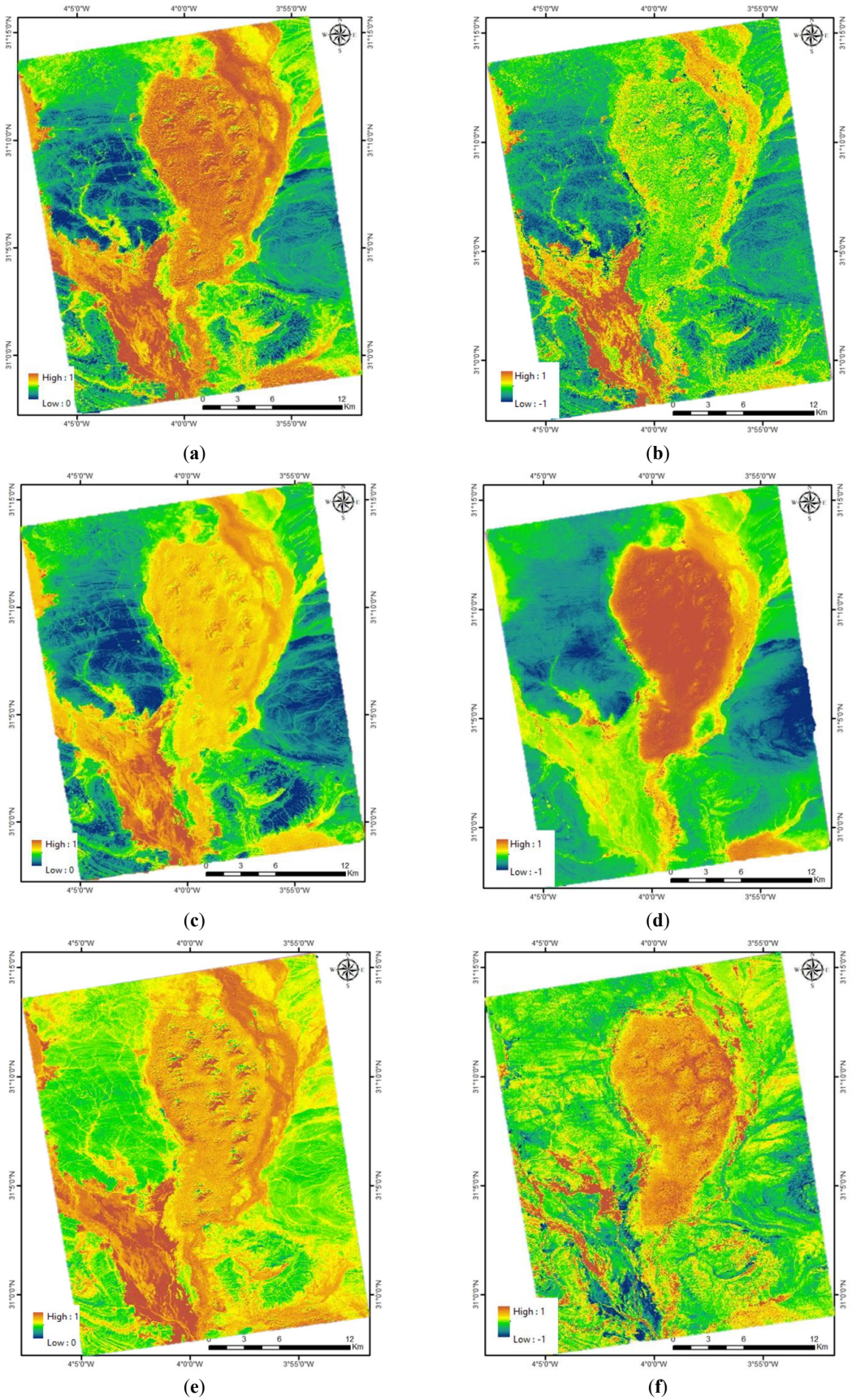

Figure 3. Spatial comparison between sand and vegetation indices obtained from ASTER and Landsat 8 sensors: (**a**,**c**,**e**): Sand indices; (**b**,**d**,**f**): NDVI.

3. Results

3.1. Vegetation and Sand Dynamics

The analysis of NDVI and NSI derived from ASTER (2011), Landsat 8 (2014), and Landsat 8 (2025) provides valuable insights into the spatio-temporal evolution of vegetation cover and sand dynamics in the Merzouga Desert over a 14-year period. In 2011, vegetation was mainly concentrated along semi-fixed dunes, near oases, and within low-relief interdune depressions, whereas the central dune fields were largely dominated by active mobile dunes. These spatial patterns reflect the strong control exerted by topography, soil moisture availability, and aeolian processes.

By 2014, Landsat 8 imagery reveals early signs of dune stabilization in some previously bare or mobile sandy areas, particularly along dune margins and near oasis systems. This trend suggests progressive vegetation colonization and localized ecological recovery, likely supported by favorable microclimatic conditions and improved sediment stability.

The reliability of the classifications varies between datasets. ASTER (2011) achieved an overall accuracy of 75.32% with a Kappa coefficient of 0.64, while Landsat 8 (2014) showed a slightly higher overall accuracy of 78.36% and a Kappa coefficient of 0.47 (**Tables 1** and **2**). In contrast, the Landsat 8 (2025) classification exhibits a marked decline in performance, with an overall accuracy of only 59.08% and a Kappa coefficient of 0.38 (**Table 3**). This reduction reflects increasing difficulties in discriminating vegetation, stable dunes, and active dunes under arid conditions, where sparse vegetation cover and spectral similarity between sandy surfaces lead to significant class confusion.

Table 1. Users' and producers' accuracy by land cover classes for the LANDSAT image (2014).

Class	Prod. Acc. (Percent)	User Acc. (Percent)	Prod. Acc. (Pixels)	User Acc. (Pixels)
Vegetation	32.65	3.68	3534/10,823	3534/96,074
Stable dunes	68.61	95.95	75,443/109,953	75,443/78,625
Active dunes	20.85	36.87	15,794/75,763	15,794/42,833
Bare soil	78.36	89.81	128,944/164,561	128,944/143,568
Overall Accuracy (Percent)			61.95	
Kappa Coefficient (Pixels)			0.47	

Table 2. Users' and producers' accuracy by land cover classes for the ASTER (2011).

Class	Prod. Acc. (Percent)	User Acc. (Percent)	Prod. Acc. (Pixels)	User Acc. (Pixels)
Vegetation	49.55	84.09	514,390/1,038,092	514,390/611,682
Stable dunes	90.27	99.35	309,620/343,009	309,620/311,642
Active dunes	85.65	54.79	261,791/305,667	261,791/477,832
Bare soil	91.52	73.19	1,043,216/1,139,830	1,043,216/1,425,442
Overall Accuracy (Percent)			75.32	
Kappa Coefficient (Pixels)			0.64	

Table 3. Users' and producers' accuracy by land cover classes for the Landsat-8 (2025).

Class	Prod. Acc. (Percent)	User Acc. (Percent)	Prod. Acc. (Pixels)	User Acc. (Pixels)
Vegetation	17.03	5.09	1843/10,823	1843/36,206
Stable dunes	68.19	69.65	74,974/109,953	74,974/107,641
Active dunes	21.56	37.06	16,332/75,763	16,332/44,065
Bare soil	73.03	69.39	120,178/164,561	120,178/173,188
Overall Accuracy (Percent)			59.07	
Kappa Coefficient (Pixels)			0.38	

To address these limitations, the classification results were qualitatively validated using high-resolution Google Earth imagery and the official 1:100,000 geological map. This validation confirms the general spatial consistency of vegetation patches, dune fields, and bare soil units, despite the reduced quantitative accuracy observed in the 2025 dataset. Consequently, trends identified for 2025 should be interpreted with caution, particularly in a quantitative context.

3.2. NDVI and NSI Patterns

NDVI and NSI indices consistently reveal an inverse relationship between vegetation cover and dune mobility across all three periods. Areas characterized by higher NDVI values generally correspond to lower NSI values, indicating reduced sand mobility due to vegetation anchoring. Conversely, bare sand and active dune zones exhibit low NDVI and high NSI values, reflecting intense aeolian activity.

This spatial complementarity highlights the effectiveness of NDVI–NSI integration for monitoring desert surface dynamics. However, the lower classification accuracy observed in 2025 emphasizes the need for caution when interpreting subtle temporal changes, especially in sparsely vegetated environments where spectral confusion is common.

3.3. Classification Accuracy

The supervised land-cover classifications distinguished four main classes: vegetation, stable dunes, active dunes, and bare soil. ASTER (2011) and Landsat 8 (2014) produced moderate to satisfactory results, with overall accuracies of 75.32% and 78.36%, respectively, and Kappa coefficients ranging from 0.47 to 0.64. These values indicate reasonable agreement between classified maps and reference data.

However, the Landsat 8 (2025) classification shows a significant decrease in accuracy (OA = 59.08%, Kappa = 0.38), reflecting substantial misclassification among vegetation, stable dunes, and active dunes. This highlights the limitations of medium-resolution optical imagery for detecting subtle land-cover changes in arid environments without extensive field validation or complementary datasets.

3.4. Topographic Changes Derived from DEM of Difference (2011–2025) and Wind Regime Influence

The DEM of Difference (DoD) generated from the Sentinel-1–derived DEM (2025) and the ASTER GDEM (2011) reveals spatially heterogeneous elevation changes across the Merzouga dune field (**Figure 4**). Areas of positive elevation change (+1 m) are mainly concentrated on dune crests and windward slopes, indicating zones of sand accumulation. In contrast, negative elevation changes (−1 m) are predominantly observed on leeward dune flanks, interdune corridors, and along dune margins, suggesting localized erosion or sediment redistribution.

Overall, the magnitude of elevation change remains moderate, reflecting gradual geomorphic processes rather than abrupt topographic transformations. The spatial distribution of erosion and accumulation patterns is consistent with aeolian-driven dune migration processes. Sediment is preferentially eroded from exposed upwind surfaces and redeposited along dune crests and downwind slopes, resulting in limited net elevation change at the scale of the entire dune field.

The observed topographic changes are closely related to the regional wind regime. Wind data indicate that dominant winds in the Merzouga region originate mainly from the northeast (NE–ENE) and south-southwest (SSW–SW) directions, with prevailing wind speeds ranging between 10 and 30 km/h (**Figure 5**). These wind directions are well aligned with the orientation of dune ridges and the spatial patterns of sand accumulation and erosion identified in the DoD map. Stronger wind events (>30 km/h), although less frequent, likely contribute disproportionately to sand transport and dune reshaping.

Central dune fields exhibit relatively stable elevation values, suggesting a dynamic equilibrium where sediment erosion and deposition processes compensate each other over time. In contrast, dune margins and interdune corridors show more pronounced elevation variability, reflecting their sensitivity to wind-driven sediment transport and local topographic controls.

The spatial coherence between wind regime characteristics and observed elevation changes provides robust qualitative evidence of long-term aeolian control on dune dynamics in the Merzouga Desert. The integration of DoD

analysis with wind data and NDVI–NSI results enhances the understanding of geomorphological responses to vegetation recovery and sand stabilization processes, particularly along dune peripheries and interdune environments.

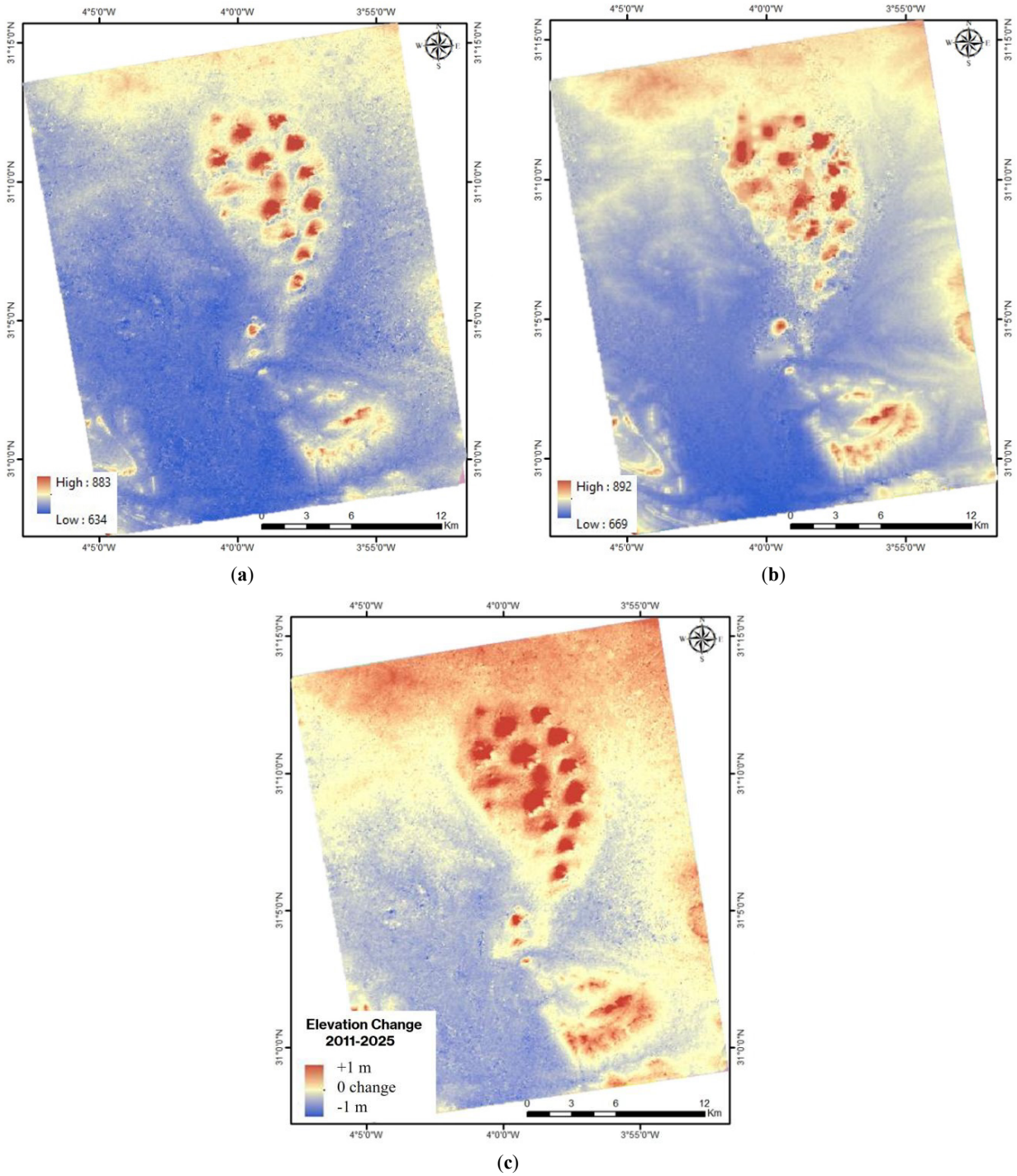

Figure 4. (**a**) ASTER Global Digital Elevation Model (GDEM) representing dune topography in 2011; (**b**) Sentinel-1 InSAR-derived Digital Elevation Model illustrating dune morphology in 2025; (**c**) DEM of Difference (DoD) showing elevation changes between 2011 and 2025, with positive values indicating sand accumulation and negative values indicating erosion or sand redistribution.

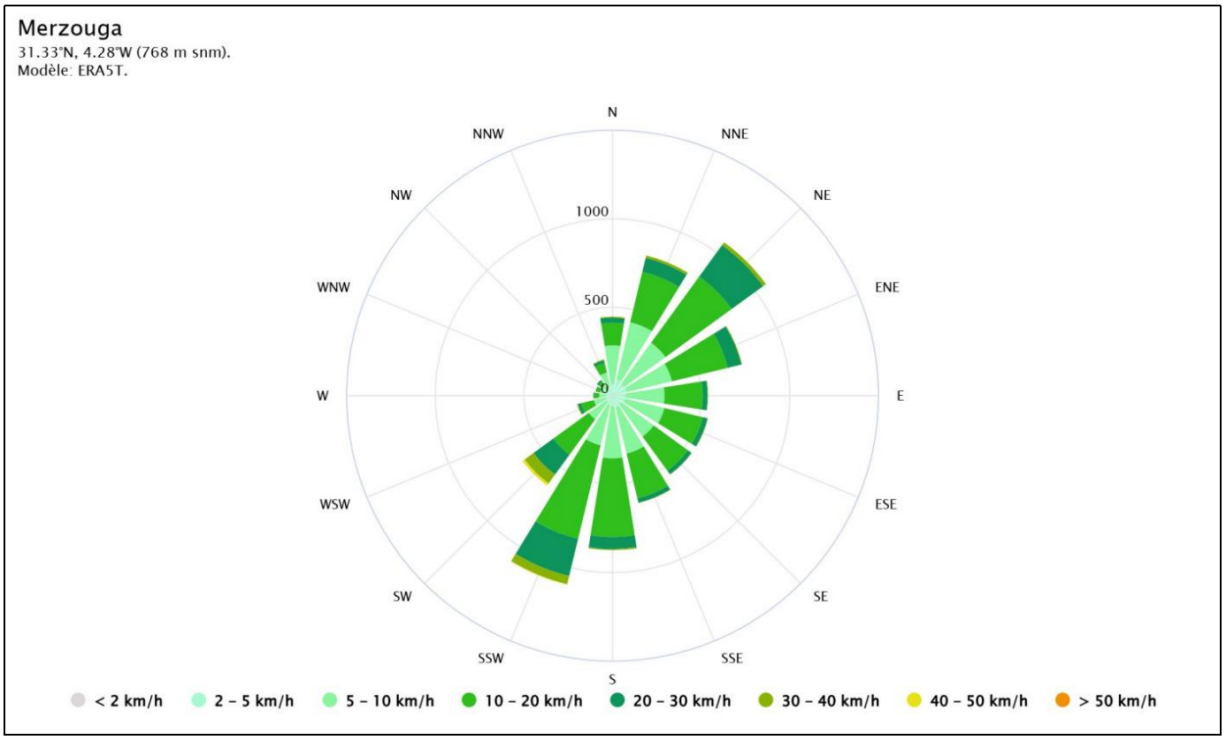

Figure 5. Directional distribution and intensity of near-surface winds at Merzouga, illustrating prevailing NE–ENE and SSW–SW winds responsible for aeolian sediment transport and dune morphology.

4. Discussion

4.1. Controls of Vegetation on Sand Mobility in an Arid Ecosystem

The results confirm that vegetation plays a fundamental ecological role in regulating sand mobility in the Merzouga Desert. Vegetated areas are preferentially associated with semi-fixed dunes, interdune depressions, and oasis margins, where local moisture availability, finer sediments, and reduced wind exposure favor plant establishment. These zones function as stabilizing elements within an otherwise highly dynamic dune system.

The inverse relationship observed between NDVI and NSI highlights the effectiveness of vegetation in reducing aeolian transport by increasing surface roughness and limiting wind velocity near the ground. Even low-density vegetation cover appears sufficient to influence sediment dynamics, supporting previous ecological studies that emphasize the disproportionate stabilizing effect of sparse vegetation in desert environments.

4.2. Topographic Responses to Aeolian Processes and Wind Regime

The DEM of Difference analysis provides geomorphological evidence of long-term aeolian control on dune evolution between 2011 and 2025. The spatial alternation between zones of sand accumulation and erosion reflects a sediment redistribution process rather than net topographic gain or loss. Accumulation on dune crests and windward slopes, combined with erosion on leeward flanks and interdune corridors, is consistent with classical dune migration mechanisms.

The strong spatial coherence between observed elevation changes and dominant wind directions (NE–ENE and SSW–SW) confirms that the regional wind regime is the primary driver of dune morphology. Although infrequent, high-energy wind events likely exert a critical influence by mobilizing large sediment volumes and reshaping dune surfaces, thereby periodically resetting ecological conditions.

Central dune fields exhibit relative topographic sta-

bility, suggesting a state of dynamic equilibrium where erosion and deposition processes compensate over time. In contrast, dune margins and interdune corridors show greater elevation variability, reflecting their heightened sensitivity to wind forcing and local surface conditions.

4.3. Vegetation–Topography Feedbacks and Ecological Significance

The integration of NDVI–NSI indicators with DoD-derived elevation changes reveals important feedback mechanisms between vegetation and topography. Areas exhibiting reduced erosion or localized accumulation often correspond to zones of higher vegetation density, particularly along dune margins and interdune corridors. Vegetation in these areas likely contributes to sediment trapping and micro-topographic stabilization, reinforcing conditions favorable for further plant colonization.

This feedback is ecologically significant because they promote spatial heterogeneity within the dune system. Rather than uniform stabilization, desert ecosystems evolve through localized processes where microhabitats play a critical role in shaping broader landscape dynamics. Such heterogeneity enhances ecological resilience by creating refugia for vegetation and limiting widespread sand mobilization.

4.4. Uncertainty, Validation, and Methodological Constraints

Despite the ecological coherence of the observed patterns, uncertainties related to classification accuracy and DEM integration must be acknowledged. The reduced accuracy of the 2025 Landsat classification highlights the difficulty of discriminating vegetation and dune stability classes in sparsely vegetated arid environments using medium-resolution optical imagery.

To mitigate these limitations, qualitative validation using high-resolution Google Earth imagery and geological maps was employed, confirming the spatial consistency of major land-cover units and geomorphic features. While these validations do not eliminate uncertainty, they strengthen confidence in the interpretation of dominant spatial patterns and long-term trends.

Similarly, the use of DEMs derived from different sensors may introduce vertical bias; however, the strong spatial alignment between elevation changes, wind regime, and ecological indicators supports the robustness of the inferred aeolian processes.

4.5. Implications for Desert Ecology and Sustainable Management

From an ecological perspective, the results emphasize that dune systems are not uniformly unstable but instead exhibit spatially differentiated responses to wind forcing and vegetation dynamics. Dune margins and interdune corridors emerge as key ecological transition zones where small increases in vegetation cover can significantly reduce sand mobility.

For sustainable desert management, these findings suggest that conservation strategies should prioritize the protection and restoration of vegetation in these sensitive areas. Targeted ecological interventions in dune peripheries may enhance natural stabilization processes, reduce sand encroachment, and improve ecosystem resilience under ongoing climatic variability.

4.6. Broader Relevance and Future Research Directions

This study demonstrates the value of integrating spectral indices, topographic change detection, and wind data for understanding desert ecosystem dynamics. While methodological limitations remain, the combined approach provides a comprehensive framework for assessing vegetation–sand interactions in arid environments.

Future research should focus on multi-sensor integration, higher-resolution DEMs, and field-based measurements to better quantify sediment fluxes and vegetation effects. Such efforts are essential for advancing ecological monitoring and informing adaptive management strategies in desert regions facing increasing environmental pressures.

5. Conclusions

This study provides an integrated ecological and geomorphological assessment of dune dynamics in the Merzouga Desert over the period 2011–2025 by combining

spectral indices (NDVI and NSI), supervised land-cover classification, topographic change detection using DEM of Difference, and wind regime analysis. The results demonstrate that vegetation, even when sparse, plays a critical role in modulating sand mobility and influencing dune stabilization processes in arid environments.

The inverse relationship between NDVI and NSI confirms the stabilizing effect of vegetation on sandy surfaces, particularly along dune margins, interdune corridors, and oasis-related environments. Topographic analyses further reveal that dune evolution is primarily governed by aeolian processes, with sediment redistribution occurring in response to dominant wind regimes rather than large-scale net elevation changes. Central dune fields exhibit dynamic equilibrium, whereas dune peripheries show greater sensitivity to both wind forcing and vegetation cover.

Despite methodological limitations related to classification accuracy and DEM integration, qualitative validation using high-resolution Google Earth imagery and geological mapping supports the ecological coherence of the observed spatial patterns. These findings highlight the importance of interpreting satellite-based analyses in arid regions as indicators of dominant processes rather than precise quantitative measures.

From an ecological perspective, the study emphasizes the role of localized vegetation–topography feedbacks in enhancing surface stability and ecosystem resilience. Dune margins and interdune environments emerge as key zones for ecological management, where targeted conservation or restoration efforts may effectively reduce sand mobility and mitigate desertification impacts.

Overall, this research demonstrates the value of multi-source remote sensing integration for understanding desert ecosystem dynamics. Future work should focus on higher-resolution datasets, multi-sensor approaches, and field-based observations to improve the quantification of vegetation effects and sediment fluxes. Such advances are essential for supporting sustainable management strategies in arid and semi-arid regions under increasing climatic and environmental pressures.

Author Contributions

N.E.H.: Conceptualization, methodology, software, and writing; H.T.: conceptualization, methodology, software, and writing; F.E.H.: reviewing, investigation, validation, and software; A.G.: visualization, resources, methodology, and reviewing. All authors have read and agreed to the published version of the manuscript.

Funding

This research received no external funding.

Institutional Review Board Statement

Not applicable.

Informed Consent Statement

Not applicable.

Data Availability Statement

Not applicable.

Acknowledgments

The authors thank the assistance of the Hassan II Academy of Sciences and Technology, Rabat (Morocco).

Conflicts of Interest

The authors declare no conflict of interest.

References

[1] Taïbi, A.N., 2017. Desertification on both sides of the world's largest desert: the Sahara and its northern and southern maxxvrgins, a context favorable to desertification? In Africa, from the Sahel and the Sahara to the Mediterranean. Ellipses Publishing: Paris, France. pp. 259–270. (in French)

[2] Middleton, N., 2024. Impacts of sand and dust storms on food production. Environmental Research: Food Systems. 1(2), 022003. DOI: https://doi.org/10.1088/2976-601X/ad63ac

[3] United Nations, 2015. Transforming Our World: The 2030 Agenda for Sustainable Development. UN: Ge-

neva, Switzerland.

[4] United Nations, 1994. United Nations: Convention to Combat Desertification in those Countries Experiencing Serious Drought and/or Desertification, Particularly in Africa. International Legal Materials. 33(5), 1328–1382. DOI: https://doi.org/10.1017/S0020782900026711

[5] Bakr, N., Weindorf, D.C., Bahnassy, M.H., et al., 2012. Multi-temporal assessment of land sensitivity to desertification in a fragile agro-ecosystem: Environmental indicators. Ecological Indicators. 15(1), 271–280. DOI: https://doi.org/10.1016/j.ecolind.2011.09.034

[6] Van Den Elsen, E., Jetten, V., 2015. Combatting desertification using a multidisciplinary approach. CATENA. 128, 211–213. DOI: https://doi.org/10.1016/j.catena.2014.10.001

[7] Stringer, L.C., 2008. Reviewing the International Year of Deserts and Desertification 2006: What contribution towards combating global desertification and implementing the United Nations Convention to Combat Desertification? Journal of Arid Environments. 72(11), 2065–2074. DOI: https://doi.org/10.1016/j.jaridenv.2008.06.010

[8] Santini, M., Caccamo, G., Laurenti, A., et al., 2010. A multi-component GIS framework for desertification risk assessment by an integrated index. Applied Geography. 30(3), 394–415. DOI: https://doi.org/10.1016/j.apgeog.2009.11.003

[9] De Pina Tavares, J., Baptista, I., Ferreira, A.J.D., et al., 2015. Assessment and mapping the sensitive areas to desertification in an insular Sahelian mountain region Case study of the Ribeira Seca Watershed, Santiago Island, Cabo Verde. CATENA. 128, 214–223. DOI: https://doi.org/10.1016/j.catena.2014.10.005

[10] Xu, D., Song, A., Tong, H., et al., 2016. A spatial system dynamic model for regional desertification simulation – A case study of Ordos, China. Environmental Modelling & Software. 83, 179–192. DOI: https://doi.org/10.1016/j.envsoft.2016.05.017

[11] Hesp, P.A., 1989. A review of biological and geomorphological processes involved in the initiation and development of incipient foredunes. Proceedings of the Royal Society of Edinburgh. Section B. Biological Sciences. 96, 181–201. DOI: https://doi.org/10.1017/S0269727000010927

[12] Bel, G., Ashkenazy, Y., 2014. The effects of psammophilous plants on sand dune dynamics. Journal of Geophysical Research: Earth Surface. 119(7), 1636–1650. DOI: https://doi.org/10.1002/2014JF003170

[13] Wang, Y., Chu, L., Daryanto, S., et al., 2019. Sand dune stabilization changes the vegetation characteristics and soil seed bank and their correlations with environmental factors. Science of The Total Environment. 648, 500–507. DOI: https://doi.org/10.1016/j.scitotenv.2018.08.093

[14] Fan, D., Zhang, Y., Qin, S., et al., 2017. Relationships between Artemisia ordosica communities and environmental factors following sand-dune stabilization in the Mu Us desert, northwest China. Journal of Forestry Research. 28(1), 115–124. DOI: https://doi.org/10.1007/s11676-016-0289-z

[15] Hao, H.-M., Huang, Z., Lu, R., et al., 2017. Patches structure succession based on spatial point pattern features in semi-arid ecosystems of the water-wind erosion crisscross region. Global Ecology and Conservation. 12, 158–165. DOI: https://doi.org/10.1016/j.gecco.2017.11.001

[16] Liu, B., Liu, Z., Lü, X., et al., 2014. Sand burial compensates for the negative effects of erosion on the dune-building shrub Artemisia wudanica. Plant and Soil. 374(1–2), 263–273. DOI: https://doi.org/10.1007/s11104-013-1866-y

[17] Gao, F., Lv, K., Jiang, Q., et al., 2025. How did the regional water-heat distribution in oasis area vary with the different spatial patterns and structures of shelterbelt system—A case study in Ulan Buh desert oasis. Agricultural and Forest Meteorology. 362, 110345. DOI: https://doi.org/10.1016/j.agrformet.2024.110345

[18] Mayaud, J., Webb, N., 2017. Vegetation in Drylands: Effects on Wind Flow and Aeolian Sediment Transport. Land. 6(3), 64. DOI: https://doi.org/10.3390/land6030064

[19] Fensholt, R., Langanke, T., Rasmussen, K., et al., 2012. Greenness in semi-arid areas across the globe 1981–2007 — an Earth Observing Satellite based analysis of trends and drivers. Remote Sensing of Environment. 121, 144–158. DOI: https://doi.org/10.1016/j.rse.2012.01.017

[20] Wang, Y.-C., Ooi, M.K.J., Ren, G.-H., et al., 2015. Species shifts in above-ground vegetation and the soil seed bank in the inter-dune lowlands of an active dune field in Inner Mongolia, China. Basic and Applied Ecology. 16(6), 490–499. DOI: https://doi.org/10.1016/j.baae.2015.04.010

[21] Liu, B., Liu, Z., Wang, L., et al., 2014. Responses of rhizomatous grass Phragmites communis to wind erosion: effects on biomass allocation. Plant and Soil. 380(1–2), 389–398. DOI: https://doi.org/10.1007/s11104-014-2104-y

[22] Yan, Q.L., Liu, Z.M., Zhu, J.J., 2009. Temporal variation of soil seed banks in two different dune systems

in northeastern Inner Mongolia, China. Environmental Geology. 58(3), 615–624. DOI: https://doi.org/10.1007/s00254-008-1535-2

[23] Liu, B., Liu, Z., Wang, L., 2012. The colonization of active sand dunes by rhizomatous plants through vegetative propagation and its role in vegetation restoration. Ecological Engineering. 44, 344–347. DOI: https://doi.org/10.1016/j.ecoleng.2012.04.021

[24] Laporte-Fauret, Q., 2021. Role of biophysical interactions in dune dynamics in response to disturbances [PhD Thesis]. University of Bordeaux: Bordeaux, France.

[25] Delgado-Fernandez, I., Davidson-Arnott, R.G.D., Hesp, P.A., 2019. Is 're-mobilisation' nature restoration or nature destruction? A commentary. Journal of Coastal Conservation. 23(6), 1093–1103. DOI: https://doi.org/10.1007/s11852-019-00716-9

[26] Goudie, A.S., Goudie, A.M., Viles, H.A., 2021. The distribution and nature of star dunes: A global analysis. Aeolian Research. 50, 100685. DOI: https://doi.org/10.1016/j.aeolia.2021.100685

[27] Puy, A., Herzog, M., Escriche, P., et al., 2018. Detection of sand encroachment patterns in desert oases. The case of Erg Chebbi (Morocco). Science of The Total Environment. 642, 241–249. DOI: https://doi.org/10.1016/j.scitotenv.2018.05.343

[28] Pons, X., Pesquer, L., Cristóbal, J., et al., 2014. Automatic and improved radiometric correction of Landsat imagery using reference values from MODIS surface reflectance images. International Journal of Applied Earth Observation and Geoinformation. 33, 243–254. DOI: https://doi.org/10.1016/j.jag.2014.06.002

[29] Chander, G., Markham, B.L., Helder, D.L., 2009. Summary of current radiometric calibration coefficients for Landsat MSS, TM, ETM+, and EO-1 ALI sensors. Remote Sensing of Environment. 113(5), 893–903. DOI: https://doi.org/10.1016/j.rse.2009.01.007

[30] Abrams, M., Hook, S., Ramachandran, B., 2002. ASTER User Handbook. Jet Propulsion Laboratory: Pasadena, CA, USA. pp. 1–135.

[31] Smith, P.H., 2009. The Sands of Time Revisited: An Introduction to the Sand-Dunes of the Sefton Coast. Amberley Publishing: Stroud, UK.

[32] Jones, M.L.M., Sowerby, A., Rhind, P.M., 2010. Factors affecting vegetation establishment and development in a sand dune chronosequence at Newborough Warren, North Wales. Journal of Coastal Conservation. 14(2), 127–137. DOI: https://doi.org/10.1007/s11852-009-0071-x

[33] Howe, M.A., Knight, G.T., Clee, C., 2010. The importance of coastal sand dunes for terrestrial invertebrates in Wales and the UK, with particular reference to aculeate Hymenoptera (bees, wasps & ants). Journal of Coastal Conservation. 14(2), 91–102. DOI: https://doi.org/10.1007/s11852-009-0055-x

[34] Houston, J.A., 2016. Summary Report: LIFE Platform Meeting—Restoration of Sand Dune Habitats. European Commission: Zandvoort, The Netherlands.

[35] Alamusa, Su, Y., Yin, J., et al., 2023. Effect of sand-fixing vegetation on the hydrological regulation function of sand dunes and its practical significance. Journal of Arid Land. 15(1), 52–62. DOI: https://doi.org/10.1007/s40333-023-0002-y

[36] Shao, R., Zhang, B., Su, T., et al., 2019. Estimating the Increase in Regional Evaporative Water Consumption as a Result of Vegetation Restoration Over the Loess Plateau, China. Journal of Geophysical Research: Atmospheres. 124(22), 11783–11802. DOI: https://doi.org/10.1029/2019JD031295

[37] Cao, J., Alamusa, Zhang, Y.H., 2019. Deep percolation and lateral migration of water in sandy dunes. Journal of Desert Research. 39, 41–47.

[38] Yang, W., Tang, J., Liang, H., et al., 2014. Deep soil water infiltration and its dynamic variation in the shifting sandy land of typical deserts in China. Science China Earth Sciences. 57(8), 1816–1824. DOI: https://doi.org/10.1007/s11430-014-4882-8

[39] Zhong, L., Feng, X., Zhao, W., 2024. Fixing active sand dune by native grasses in the desert of Northwest China. Ecological Processes. 13(1), 77. DOI: https://doi.org/10.1186/s13717-024-00556-y

[40] Frati, D., 2022. The Refractories of the Desert: A Study of the Relationship between Gift Exchanges and the Market Economy among the Winter Residents of the La Posa Desert, Arizona. Carnets de géographes. 16. DOI: https://doi.org/10.4000/cdg.8289 (in French)

[41] Zheng, Z., Du, S., Taubenböck, H., et al., 2022. Remote sensing techniques in the investigation of aeolian sand dunes: A review of recent advances. Remote Sensing of Environment. 271, 112913. DOI: https://doi.org/10.1016/j.rse.2022.112913

[42] Smith, P.H., 1999. The Sands of Time Revisited: An Introduction to the Sand-Dunes of the Sefton Coast. National Museums and Galleries on Merseyside & Sefton Council: Liverpool, UK.

[43] Peng, L., Wan, Y., Shi, H., et al., 2023. Influence of Climate, Topography, and Hydrology on Vegetation Distribution Patterns—Oasis in the Taklamakan Desert Hinterland. Remote Sensing. 15(22), 5299. DOI:

https://doi.org/10.3390/rs15225299

[44] Yang, F., Ping, L., Ma, F., et al., 2023. Morphological evolution and migration characteristics of reticulate dunes. Journal of Desert Research, 43(1), 107–115.

[45] Mainguet, M., Cossus, L., 1980. Sand circulation in the Sahara: Geomorphological relations between the Sahara and its margins. In Palaeoecology of Africa and the Surrounding Islands. Routledge: London, UK. pp. 69–78.

[46] Wu, W., Zucca, C., Karam, F., et al., 2016. Enhancing the performance of regional land cover mapping. International Journal of Applied Earth Observation and Geoinformation. 52, 422–432. DOI: https://doi.org/10.1016/j.jag.2016.07.014

[47] Curell, G., Dowman, A., 2009. Essential Mathematics and Statistics for Science, 2nd ed. Wiley-Blackwell: Hoboken, NJ, USA.

[48] Reimann, C., Filzmoser, P., Garrett, R.G., et al., 2008. Statistical Data Analysis Explained: Applied Environmental Statistics with R, 1st ed. Wiley: London, UK. DOI: https://doi.org/10.1002/9780470987605

[49] Secu, C.V., Stoleriu, C.C., Lesenciuc, C.D., et al., 2022. Normalized Sand Index for Identification of Bare Sand Areas in Temperate Climates Using Landsat Images, Application to the South of Romania. Remote Sensing. 14(15), 3802. DOI: https://doi.org/10.3390/rs14153802

[50] Rouse, J.W., Haas, R.H., Scheel, J.A., et al., 1974. Monitoring vegetation systems with ERTS. Proceedings of the 3rd Earth Resources Technology Satellite Symposium. 1, 48–62.

[51] Kong, D., McVicar, T.R., Xiao, M., et al., 2022. phenofit : An R package for extracting vegetation phenology from time series remote sensing. Methods in Ecology and Evolution. 13(7), 1508–1527. DOI: https://doi.org/10.1111/2041-210X.13870

[52] Liu, X., Shen, H., Yuan, Q., et al., 2022. One-Step High-Quality NDVI Time-Series Reconstruction by Joint Modeling of Gradual Vegetation Change and Negatively Biased Atmospheric Contamination. IEEE Transactions on Geoscience and Remote Sensing. 60, 1–17. DOI: https://doi.org/10.1109/TGRS.2021.3124798

[53] Lee, S.J., Youn, Y., Sohn, E., et al., 2022. A real-time correction of the underestimation noise for GK2A daily NDVI. Korean Journal of Remote Sensing. 38(6_1), 1301–1314. (in Korean)

[54] Eun, J., Kim, S.H., Kim, T., 2021. Analysis of the cloud removal effect of Sentinel-2A/B NDVI monthly composite images for rice paddy and high-altitude cabbage fields. Korean Journal of Remote Sensing. 37(6_1), 1545–1557. (in Korean)

[55] Kooistra, L., Berger, K., Brede, B., et al., 2024. Reviews and syntheses: Remotely sensed optical time series for monitoring vegetation productivity. Biogeosciences. 21(2), 473–511. DOI: https://doi.org/10.5194/bg-21-473-2024

[56] Xiao, J., Huang, K., Lin, Y., et al., 2022. Assessing Vegetation Phenology across Different Biomes in Temperate China—Comparing GIMMS and MODIS NDVI Datasets. Remote Sensing. 14(23), 6180. DOI: https://doi.org/10.3390/rs14236180

[57] Chen, Y., Cao, R., Liu, S., et al., 2024. A new deep learning-based model for reconstructing high-quality NDVI time-series data in heavily cloudy areas: fusion of Sentinel 1 and 2 data. International Journal of Digital Earth. 17(1), e2407941. DOI: https://doi.org/10.1080/17538947.2024.2407941

[58] Şenel, T., Kanmaz, O., Bektas Balcik, F., et al., 2023. Assessing Phenological Shifts of Deciduous Forests in Turkey under Climate Change: An Assessment for Fagus orientalis with Daily MODIS Data for 19 Years. Forests. 14(2), 413. DOI: https://doi.org/10.3390/f14020413